Thermal Fluid and Chemical Analysis of Ionized Air Test Injection for Cold Start Emission Mitigation

Izudin Delić[1,*]

[1]*Faculty of Mechanical Engineering, University of Tuzla, Bosna and Herzegovina*

Abstract: The cold start period of an internal combustion engine (ICE) is a dominant source of hydrocarbon (HC) and carbon monoxide (CO) emissions. This paper analyzes an innovative ejector system for distributing ionized air directly into the exhaust system to accelerate pollutant oxidation. Analytical results demonstrate that the system achieves an ejection ratio ω = 0.187 at an exhaust temperature of 450 K, while a 180 W heater provides the necessary thermal compensation to maintain the mixture temperature above the 380 K activation threshold. Experimental validation confirmed that ionized air initiates low-temperature oxidation (afterburning), evidenced by a 5.0% vol. increase in CO_2 concentration. This synergistic fluid-thermal and chemical strategy reduces the catalyst's critical inactivity period from 120 s to 85 s, offering highly efficient method for meeting stringent emission regulations.

Keywords: Ionized air, Cold start, Ejector ratio, Non-thermal activation, Emission, Oxidation.

INTRODUCTION

The combustion of fuel in a gasoline engine produces exhaust gases that are more or less harmful to the environment and humans [1-5]. If complete combustion were to occur in engines, the result of such operation would be only conditionally harmless carbon dioxide (CO_2), water vapor (H_2O) and nitrogen (N_2). Of the harmful components, emissions of carbon monoxide (CO), hydrocarbons (HC) and nitrogen oxides (NO_X) in spark-ignition engines (Otto gasoline engines) are regulated by law. Although their share in the total amount of exhaust gases generated by combustion is very small (as shown in the diagram in the figure, data taken from [6]), these components cause problems for human health and environmental pollution.

Driven by emission regulations, catalytic converters significantly reduce exhaust emissions but maintain functional drawbacks during cold start modes, as they do not operate efficiently until reaching an optimal temperature of around 400 °C [7-9]. Consequently, at temperatures between 200 °C and 300 °C, the catalytic materials (platinum, palladium, and rhodium) are either inactive or exhibit extremely low conversion rates [10]. As a rule, it takes several minutes (usually 2 to 5 minutes, depending on the ambient temperature and engine load) of engine operation for the exhaust gases to heat up the catalytic converter structure and the heat to be transferred to the ceramic monolith of the catalyst [11]. Low ambient temperatures extend the "cold start" period, so the period of high HC and CO emissions is longer, making it the most critical part of vehicle environmental control. Research shows that HC emissions can be several times (even 3 to 4 times) higher at a temperature of 0°C or -7°C compared to starting the engine at 20°C [12-16].

During the cold start of an engine, a greater quantity of fuel (a rich mixture λ< 1) is injected to ensure reliable engine operation. Since there is not enough oxygen, part of the fuel does not burn completely, and is emitted as HC. Due to the lack of oxygen, combustion is incomplete, so the rich mixture further increases the CO concentration [17]. Often, in the engine operating interval, the cold start period is relatively short, but it significantly contributes to the total pollution per driving cycle. Therefore, newer standards, such as EURO 6, place a clear emphasis on reducing emissions during this period. During the warm-up period, the engine operates in an unstable regime, which further complicates emission control. For proper and reliable operation, the catalytic device requires a stoichiometric ratio of λ= 1 to have optimal conversion of NOX, CO and HC, and this cannot be achieved during cold start. Manufacturers are developing increasingly advanced exhaust gas aftertreatment systems to meet high regulatory criteria [18]. Current available solutions require placing the catalyst closer to the engine (for faster warm-up) or using electric monolithic heating [19, 20]. One possible way to reduce pollutant emissions during the cold start period is the controlled introduction of a reactant (*e.g.* ionized air) into the exhaust system.

The significance of researching air ionization for the treatment of harmful gases is underscored by recent academic literature, which highlights its high efficiency in neutralizing complex pollutants [1, 2]. As demonstrated by these studies, this technology not only provides a solution for industrial emissions but also paves the way for sustainable air quality management through energy-efficient non-thermal

*Address correspondence to this author at the Faculty of Mechanical Engineering, University of Tuzla, Bosna and Herzegovina;
E-mail: izudin.delic@untz.ba

Received on 16-11-2025 Accepted on 20-12-2025 Published on 27-12-2025

E-ISSN: 2409-9848/25

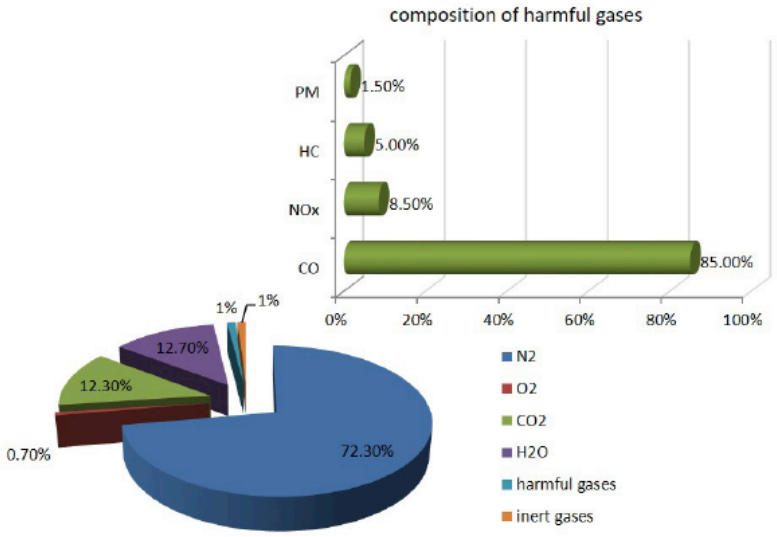

Figure 1: Composition of exhaust gases of an internal combustion engine - gasoline engine.

plasma processes, directly addressing global environmental challenges such as the reduction of NO_x and VOC emissions. [21, 22].

2. MATERIALS AND METHODS

2.1. Air Ionization Process

Ionization is a process of electron-atom interaction, in which an electron can expel another electron from an atom or join an atom as shown in Figure **2** [23, 24].

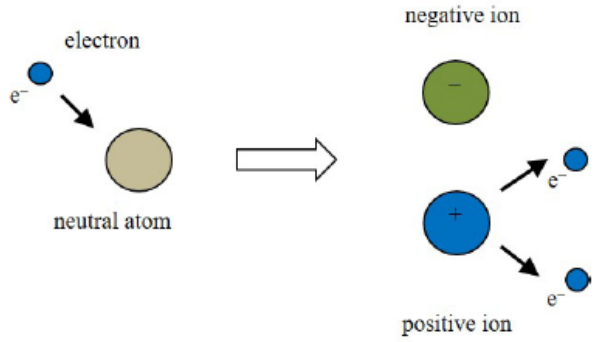

Figure 2: The process of ionization of gas atoms.

The ionization process caused by the electric field occurs when the gas passes between the positive and negative electrodes. Depending on the polarity of the electrode, gas atoms or molecules can lose or gain an electron when they come into contact with the electrode surface. In order to start this process, it is necessary to enable a high electric field density (of the order of several kV/m). The shape of the electrode itself is important, because a sharp or slightly curved electrode concentrates a stronger field, enabling ionization in space, Figure **3**.

Accordingly, only the ionization rate decreases at lower field intensity. At higher pressures and fluid flows between the electrodes, greater electrical energy is required to initiate the ionization process. Typically, in an ionizer device, a high DC voltage is applied to a needle electrode to create a corona discharge. Due to the action on the surrounding air molecules, an exchange of electrons occurs and negative ions are formed.

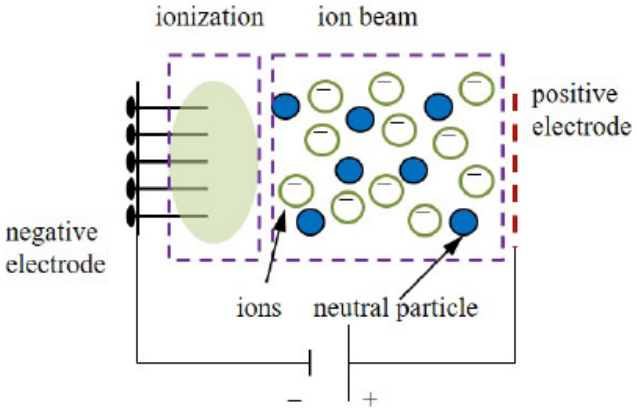

Figure 3: The process of generating negative ions on the electrode.

Corona discharge generated in this way occurs when the gradient of the electric field strength around the electrode exceeds a threshold value. The appearance and intensity of the corona depend on the voltage, shape and spacing of the electrodes, as well as on the density and temperature of the gas. The electron ejection process is stronger on needle-shaped electrodes with a small radius of curvature. Although corona can occur with both polarities, the negative corona is more stable, which allows a higher voltage to be applied to the ionizing electrode [25, 26].

2.2. Motivation for Intervention

To quantify the need for intervention, a characteristic emission profile diagram was generated (Figure **4**).

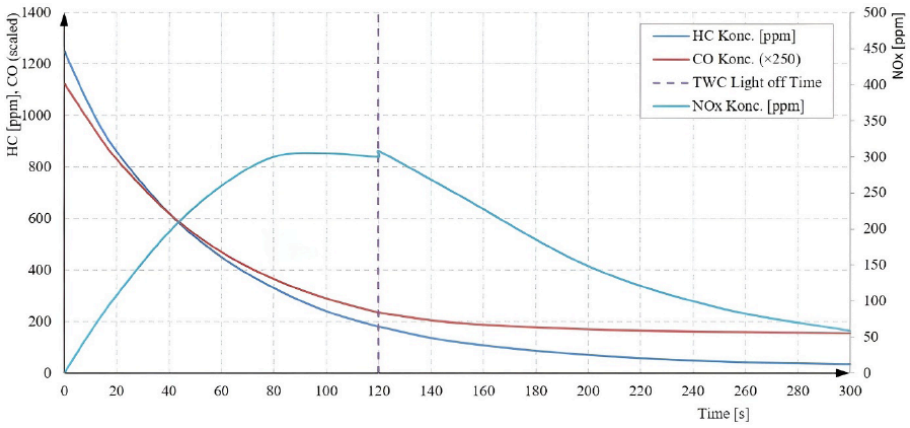

Figure 4: Exhaust gas emission profile during old start.

The curves were generated using standard exponential functions to model the cooling/heating process (*i.e.*, the concentration decay):

HC curve: $$HC(t) = HC_{top} \cdot e^{-t/\tau_{HC}} + HC_{steady} \quad (1)$$

CO curve: $$CO(t) = CO_{top} \cdot e^{-t/\tau_{CO}} + CO_{steady} \quad (2)$$

Where

$\tau_{HC} \approx 50\ s$ (Rapid drop, characteristic of condensation and a rapid increase in engine temperature)

$\tau_{CO} \approx 80\ s$ (Slower drop, because CO depends on the enrichment of the mixture, which decreases more slowly)

NOx curve: Combination of rise (engine warm-up) and fall (after catalytic converter activation).

These mathematical constants (τ_{HC}, τ_{CO}) were chosen to qualitatively mimic the profiles from academic studies on exhaust gas emissions, but they are abstract and serve only as an illustration.

The 'light-off' time, defined as the point where the catalyst achieves 50 % conversion efficiency, typically falls between 60 s and 150 s during the test norm FTP-75, confirming the 120 second period.

2.3. Ion-Initiated Oxidation

For the purposes of this research, we are interested in targeted oxidation reactions enabled by negative ions. The advantage of using ionized air in exhaust gas after treatment is the cold oxidation of hydrocarbons and carbon monoxide. Here, ions (O_2^-, O^-, N_2^+) serve as initiators of chain reactions. The use of ionized air for this purpose enables reactions to be carried out for the rapid conversion of CO to CO2. This is important because high concentrations of CO are generated due to the rich fuel mixture during cold engine starts.

CO oxidation: $$2CO + O_2 \rightarrow 2CO_2 \quad (3)$$

Hydrocarbons (HC), represented by C_XH_Y, are more complex, but the end result is complete combustion.

HC oxidation: $$C_xH_y + (x + y/4)O_2 \rightarrow xCO_2 + (y/2)H_2O \quad (4)$$

The primary role of the ionization process is to activate oxygen molecules (O_2) from the air and thus generate highly reactive oxygen that reacts with pollutant molecules.

Oxygen activation:

$$e^- + O_2 \rightarrow O_2^- \quad \text{(Negative molecular ion)} \quad (5)$$

$$e^- + O_2 \rightarrow O + O^- \quad \text{(Negative atomic ion)} \quad (6)$$

Active forms of oxygen created in this way react with pollutants much faster than neutral oxygen can at low temperatures.

Ionic catalysis of CO:

$$CO + O^- \rightarrow CO_2 + e^- \quad (7)$$

2.4. Defining the Ejection Problem

Adding a secondary fluid to the exhaust system is a challenge due to the overpressure that exists inside. Conventional systems require external pumps or compressors, which increases the weight, complexity and energy consumption of the vehicle [27]. As a solution, the implementation of an ejector system that would use the kinetic energy of the exhaust gases (in this case the primary fluid) to draw in and mix the secondary fluid is imposed.

An ejector is a passive fluidic device, without moving parts, designed to transfer kinetic energy from one fluid (primary flow) to another fluid (secondary flow), thereby achieving the suction of the secondary fluid. The ejector uses the available kinetic energy of

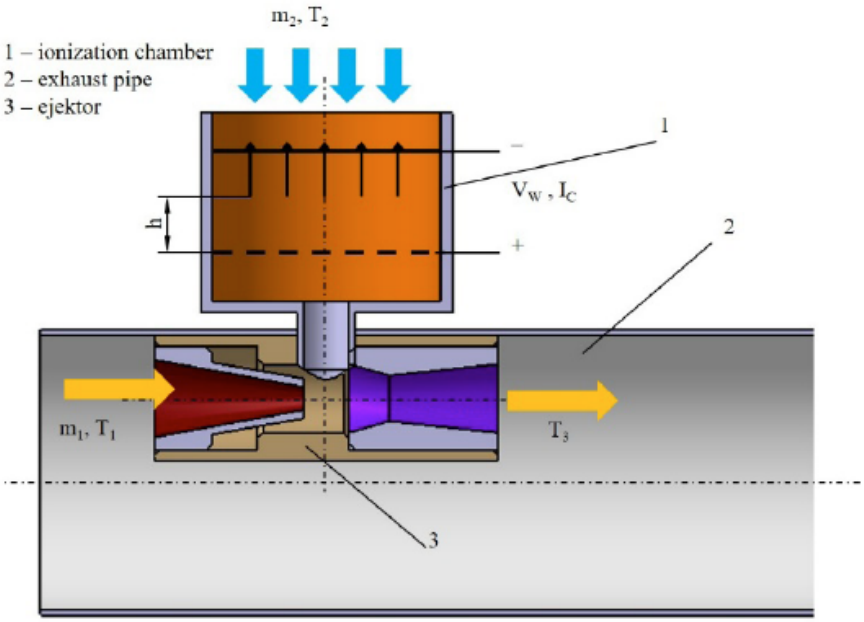

Figure 5: The constituent parts of the ejector.

the high-speed exhaust gases as the primary fluid [28]. In the context of this work, the ejector serves to implement an energy-efficient solution for suctioning ionized air into the exhaust system. The components of the ejector, shown in Figure **5**, are:

The introduction of an ejector into the exhaust system changes the need for compressors or pumps that would require a portion of the engine power. The mass and energy transfer process takes place between the exhaust gases and the ionized air. The geometry of the ejector is not the subject of this study. The efficiency of the primary fluid energy utilization process in the ejector is defined by the ejection ratio (ω) [29], given by the expression:

$$\omega = \frac{\dot{m}_2}{\dot{m}_1} \tag{8}$$

Assuming that the ejector geometry can provide a flow of ionized air sufficient for complete interaction with pollutants in the exhaust system, we will consider only the operational parameters of the ejector. Therefore, the analysis of the process parameters of the ejector affects the operational feasibility and overall efficiency of the system for reducing harmful components in the exhaust gases.

The coefficient of utilization for the ejector is denoted by Ψ and is given by the expression:

$$\Psi\left(\frac{\dot{m}_2}{\dot{m}_1}\right) = \frac{k_3 \cdot \frac{\left[\frac{R_1+\frac{\dot{m}_2}{\dot{m}_1}R_2}{\left(1+\frac{\dot{m}_2}{\dot{m}_1}\right)}\right]\left[\frac{c_{p1}\cdot T_1+\frac{\dot{m}_2}{\dot{m}_1}c_{p2}\cdot T_2}{\left(1+\frac{\dot{m}_2}{\dot{m}_1}\right)\cdot c_{p2}}\right]}{k_3-1}\left[1-\left(\frac{p_2}{p_3}\right)^{\frac{k_3-1}{k_3}}\right]}{\frac{k_1\cdot R_1\cdot T_2\cdot\left[1-\left(\frac{p_2}{p_1}\right)^{\frac{k_1-1}{k_1}}\right]}{k_1-1}} \tag{9}$$

And the temperature of the mixture of ionized air and exhaust gas, *i.e.*, the temperature at the ejector assembly's outlet, is given by the expression:

$$T_3\left(\frac{m_2}{m_1}\right) = \frac{c_{p1}\cdot T_1+\frac{\dot{m}_2}{\dot{m}_1}c_{p2}\cdot T_2}{\left(1+\frac{\dot{m}_2}{\dot{m}_1}\right)\cdot c_{p2}} \tag{10}$$

Where:

T_i Absolute temperatures of the gases at rest [K]

R_i Gas constants [J/kgK]

c_{pi} Specific heat capacities of the gas at constant pressure [J/kgK]

ω Ratio of the mass flow rates of the entrained and motive gas [-].

Index 1 refers to the motive gas, index 2 refers to the entrained gas, and index 3 refers to the mixture of the motive and entrained gas at the ejector outlet.

2.5. Experimental Set-Up

Figure **6** shows the experimental set-up. The experiment simulates the cold start phase of an internal combustion engine and the interaction of ionized air with exhaust gases. The equipment consists of four main parts: generator/aggregate, ionization chamber, power supply and measurement/analysis system (The flue gas composition was monitored with a Testo 350 S analyzer, which provided real-time data on the concentrations of various pollutants during the experiment).

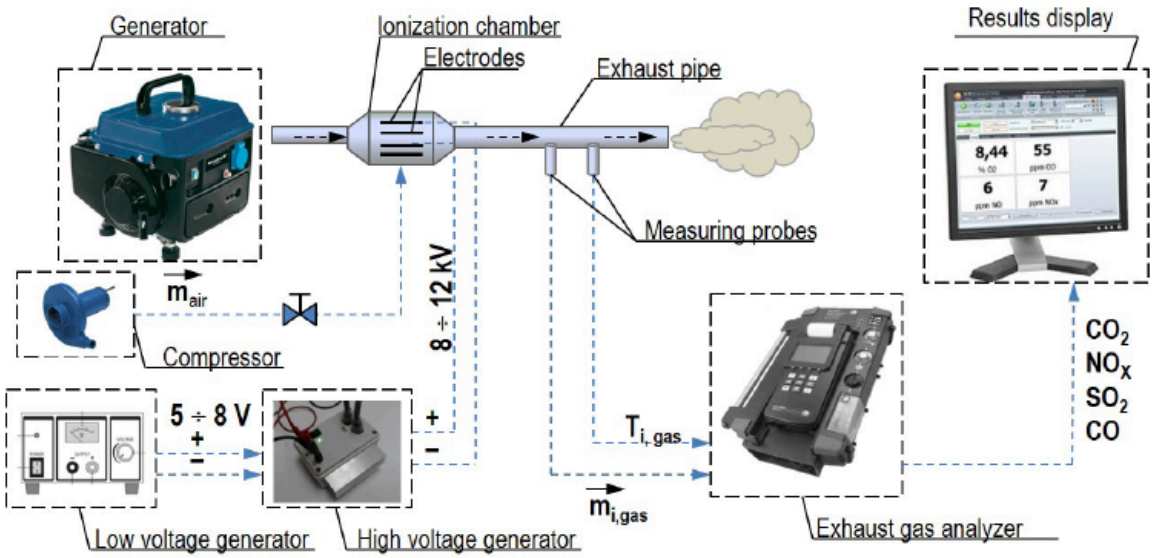

Figure 6: Experimental set-up for testing the interaction of ionized air and exhaust gas.

The aggregate is a power generation unit, model Einhell BT-PG 850, 63 cm^3. The system requires two power sources: High voltage generator for the ionization electrodes and Low voltage generator (5V) for powering the high voltage generator assembly (8 kW). Conversion Chain is: 5V DC → Pulsed signal (555 timer) → MOSFET Switch → Ignition Coil (Voltage Step-up) → HV Diode → -8kV at the needle. Air supply via compressor to the ionization chamber (210 l/min). The distance between the air ionization electrodes is 6 mm.

3. RESULTS AND DISCUSSIONS

3.1. Experimental Results

The diagram, shown in Figure **7**, shows the change in temperature and concentration over the interaction time. Jumps in temperature values can be observed that coincide with the change in CO2 concentration. This phenomenon indicates the interaction of ionized air and corona discharge with exhaust gas and the occurrence of afterburning in the exhaust system.

The experiment had to be terminated when the exhaust gas temperature at the sampling point exceeded 100°C due to these combustion events, in order to protect the ionization assembly housing from thermal damage. The housing is made using a 3D printing technique from PLA (polylactic acid) filament, which cannot withstand high temperatures.

By applying voltage to the electrodes, an electric field was established, at certain moments an electric arc was established or sparking occurred at the electrode. This phenomenon negatively affects the stability of the corona discharge and reduces the formation of negative ions. Since there is a significant

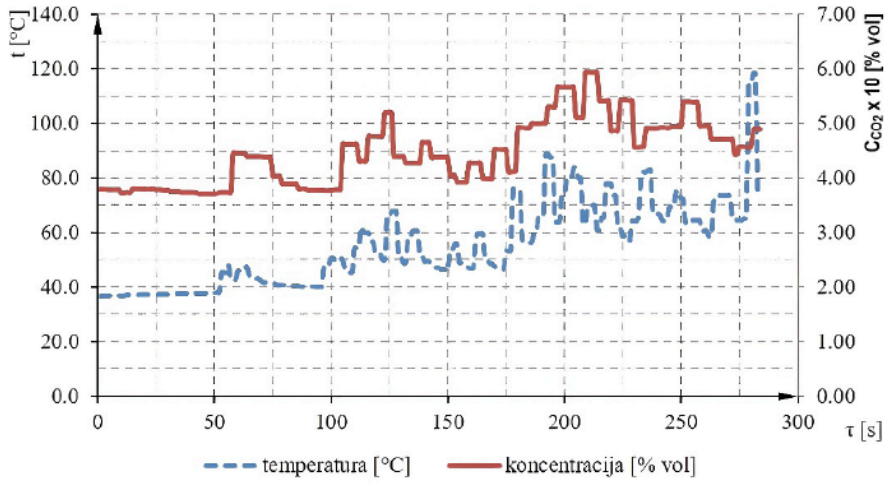

Figure 7: Temperature changes at elevated voltage in parallel with CO_2 concentration.

amount of hydrocarbons in the cold start, detonations occurred when the exhaust gas came into contact with the electric field. This represents an unplanned but relevant chemical activation and a rapid temperature rise.

The observed increase in CO_2 concentration (reaching 5.0 % vol.) serves as a proxy measurement for the oxidation of hydrocarbons and carbon monoxide. Since CO_2 and heat are the primary products of HC/CO oxidation, the simultaneous jump in temperature and CO_2 levels necessarily indicates a reduction in pollutant concentrations. This relationship confirms that the ionized air successfully initiated the afterburning process, effectively shifting the pollutant conversion threshold even before the catalyst reached its full operational temperature.

3.2. Analytical Results

During the cold start period, the operating regime is characterized by low engine speed and minimal load. This period is particularly sensitive for emission control due to the cold state of the catalytic device. Rapid addition of negative ions is necessary to achieve instantaneous thermal or chemical activation. The primary fluid (exhaust gas) provides the driving force, and its parameters are adopted from the engine operating conditions [30]. Table **1** and Table **2** list the parameters of the primary and secondary fluid.

Table 1: Primary Fluid Parameters

Parameter	Regime - Cold Start
Temperature (T_p)	approx. 400 - 550 K
Inlet pressure (p_p)	approx. 105 - 110 kPa
Mass flow (m_p)	lower

The secondary fluid is the entrained air, thus its inlet conditions are nearly constant.

In order to keep the mixture temperature (T_3) within an acceptable range, even at low temperatures (-7°C and 0°C), the air being ionized and entering the exhaust system must be preheated. Cold air prolongs the cold-start period and the duration of increased pollutant emissions. The maximum acceptable heater power for short-term use during cold start is approximately 180 W at a voltage of 12 V. The temperature difference (ΔT) achievable with a 180 W heater and the maximum ejector ratio is calculated from:

$$\Delta T = \frac{P}{\dot{m}_2 \cdot c_{p2}} \tag{11}$$

Based on the parameters in the Table **1** and Table **2**, and assuming the maximum ejector ratio (ω = 0.2), the resulting temperature difference Δ T = 22.39°C (or 22.39 K).

By preheating the ionization air and taking into account the temperature threshold for the start of catalytic converter operation, a diagram is generated that illustrates the influence of the fluid temperature on the ejector ratio, Figure **8**.

4. CONCLUSIONS

The analysis of the system for adding ionized air during a cold start using an ejector was carried out, supported by thermofluid calculations and emission profile modeling. It confirms the feasibility and significant potential of the proposed solution for reducing pollution.

The research on the implementation of an ejector system for ionized air injection confirmed the technical feasibility and environmental potential of the proposed solution through the following numerical and experimental findings:

- Fluid and thermal efficiency: The analysis demonstrated that the ejector system maintains a stable suction flow without the need for external power sources. At a characteristic catalyst inactivity temperature of 450 K, an ejection ratio of ω = 0.187 was achieved. By integrating a 180 W heater, the mixture temperature (T_3) was raised above the activation threshold of 380 K, thereby preventing thermal cooling of the catalytic monolith caused by the introduction of secondary air.

Table 2: Secondary Fluid Parameters

Parameter	Value/Condition	Remark
Temperature (T_s)	293 K (Const.)	The ambient temperature is approximately 20°C, and heating due to ionization is neglected.
Inlet pressure (p_s)	101.325 kPa (Const.)	Atmospheric pressure. This is the pressure of the static chamber from which the air is entrained.
Mass flow (m_s)	Variable	This is the resulting output! Mass flow is entrained passively, and its value defines the ejector ratio ω.

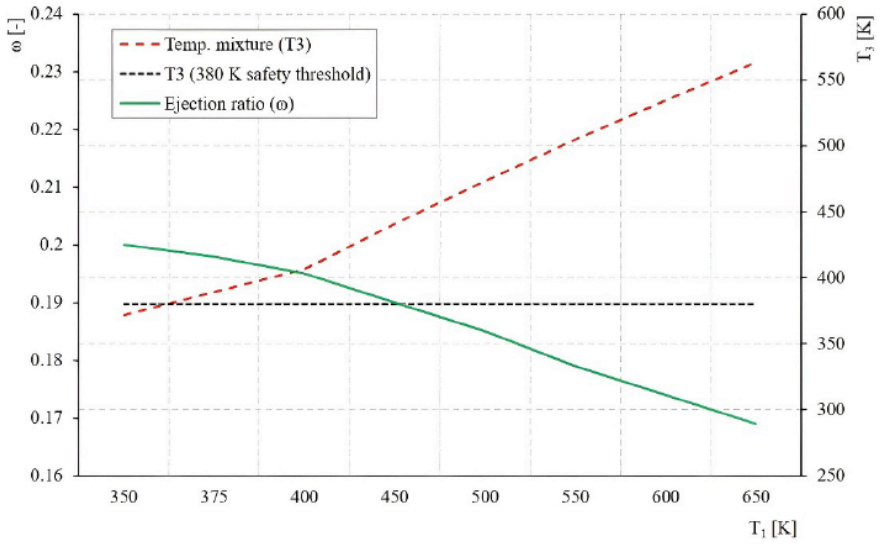

Figure 8: Ejector performance (ω and T_3) during engine warm-up period.

- Experimental confirmation of oxidation: Afterburn tests provided direct evidence of ionic activation. Activating the ionizer resulted in an instantaneous jump in CO_2 concentration up to 5.0 % vol., accompanied by a sharp rise in exhaust gas temperature. These data confirm that free radicals and ions initiate the oxidation of unburned fuel at temperatures significantly lower than those required for conventional thermal oxidation.

- Reduction of the critical period: By combining thermal compensation and ionic catalysis, the theoretical pollutant conversion curve was shifted to the left on the timeline. Calculations indicate a reduction in the catalyst inactivity period from 120 s to approximately 85 s, representing a 29 % reduction in the critical emission phase.

Although the results are promising, further research on an engine test bench is required for a precise quantification of HC and CO reduction. Future work will focus on optimizing the ionization chamber geometry to eliminate unwanted arcing and maximize the density of negative ions. The synergy of ejector technology and low-temperature chemical activation represents a sustainable strategy for meeting future, more stringent emission standards.

4.1. Limitations

While the results of this study demonstrate the potential of ionized air for cold-start emission mitigation, several limitations inherent to the preliminary nature of the experimental and modeling setup must be acknowledged.

Material constraints: The ionization chamber housing was manufactured using PLA-based 3D printing. This limited the duration of experimental runs, as the housing could not withstand exhaust temperatures exceeding 100 °C. This prevented long-term stability testing of the corona discharge under high-thermal loads.

Scaling and engine variability: The experiments were conducted on a small-scale 63 cm^3 power generation unit. While the fundamental fluid dynamics remain similar, the mass flow rates and chemical complexity of exhaust gases from a multi-cylinder passenger vehicle engine may differ significantly, potentially affecting the ejection ratio (ω) and ion survival rates.

Arcing and discharge stability: As noted in the results, high concentrations of hydrocarbons during the initial seconds of the cold start led to occasional arcing and unplanned detonations within the ionization chamber. This indicates that the current electrode geometry and insulation require further refinement to ensure stable non-thermal plasma generation.

4.2. Future Work

Future research will focus on transitioning from a proof-of-concept prototype to a robust automotive-grade system. Key directions include:

- Developing ionization chambers using ceramic or high-grade stainless steel to allow for continuous operation at full exhaust temperatures.

- Utilizing Computational Fluid Dynamics (CFD) to optimize the internal geometry of the ejector and ionization circuit, aiming to maximize the ejection

ratio while minimizing the pressure drop in the exhaust tract.

- Conducting tests on a standard engine dynamometer (test bench) with high-precision gas analyzers to quantify the reduction of specific HC species and CO, aligning with the FTP-75 or WLTP driving cycles.

CONFLICTS OF INTEREST

The author declared no conflicts of interest.

REFERENCES

[1] Gulia S, Nagendra SS, Khare M, Khanna I. Urban air quality management-A review. Atmos. Pollut. Res. 2015; 6(2): 286-304. https://doi.org/10.5094/APR.2015.033

[2] Nagpure AS, Gurjar BR, Kumar P. Impact of altitude on emission rates of ozone precursors from gasoline-driven light-duty commercial vehicles. Atmos. Environ. 2011; 45(7): 1413-7. https://doi.org/10.1016/j.atmosenv.2010.12.026

[3] Shah IH, Zeeshan M. Estimation of light duty vehicle emissions in Islamabad and climate co-benefits of improved emission standards implementation. Atmos. Environ. 2016; 127: 236-43. https://doi.org/10.1016/j.atmosenv.2015.12.012

[4] Kampa M, Castanas E. Human health effects of air pollution. Environ. Pollut. 2008; 151(2): 362-7. https://doi.org/10.1016/j.envpol.2007.06.012

[5] Twigg MV. Catalytic control of emissions from cars. Catal. Today. 2011; 163(1): 33-41. https://doi.org/10.1016/j.cattod.2010.12.044

[6] Dziubak T, Karczewski M. Experimental Studies of the Effect of Air Filter Pressure Drop on the Composition and Emission Changes of a Compression Ignition Internal Combustion Engine. Energies. 2022; 15(13): 4815. https://doi.org/10.3390/en15134815

[7] Samuel S, Morrey D, Fowkes M, Taylor DHC, Garner CP, Austin L. Real-world performance of catalytic converters. Proceedings of the Institution of Mechanical Engineers, Part D: Journal of Automobile Engineering. 2005; 219(7): 881-888. https://doi.org/10.1243/095440705X28349

[8] Saliba G, Saleh R, Zhao Y, Presto AA, Lambe AT, Frodin B et al. Comparison of gasoline direct-injection (GDI) and port fuel injection (PFI) vehicle emissions: emission certification standards, cold-start, secondary organic aerosol formation potential, and potential climate impacts. Environ Sci Technol. 2017; 51(11): 6542-6552. https://doi.org/10.1021/acs.est.6b06509

[9] Puértolas B, Navlani-García M, García T, Navarro MV, Lozano-Castelló D, Cazorla-Amorós D. Optimizing the performance of catalytic traps for hydrocarbon abatement during the cold-start of a gasoline engine. J. Hazard. Mater. 2014; 279: 527-36. https://doi.org/10.1016/j.jhazmat.2014.07.042

[10] Korin R, Reshef D, Tshernichovesky E, Sher E. Reducing cold-start emission from internal combustion engines by means of a catalytic converter embedded in a phase-change material. Proc Inst Mech Eng Part D: J Automob Eng. 1999; 213(6): 575-83. https://doi.org/10.1243/0954407991527116

[11] Reiter MS, Kockelman KM. The problem of cold starts: A closer look at mobile source emissions levels. Transp Res Part D-Transp Environ. 2016; 43: 123-32. https://doi.org/10.1016/j.trd.2015.12.012

[12] Will F, Boretti A. A new method to warm up lubricating oil to improve the fuel efficiency during cold start. SAE technical paper 2011-01-0318; 2011.

[13] Yusuf AA, Inambao FL. Effect of cold start emissions from gasoline-fueled engines of light-duty vehicles at low and high ambient temperatures: Recent trends. Case Stud Therm Eng. 2019; 14: 100417. https://doi.org/10.1016/j.csite.2019.100417

[14] Bielaczyc P, Szczotka A, Woodburn J. The effect of a low ambient temperature on the cold-start emissions and fuel consumption of passenger cars. Proc Inst Mech Eng Part D: J Automob Eng. 2011; 225(9): 1253-64. https://doi.org/10.1177/0954407011406613

[15] Chen L, Liang Z, Zhang X, Shuai S. Characterizing particulate matter emissions from GDI and PFI vehicles under transient and cold start conditions. Fuel. 2017; 189: 131-40. https://doi.org/10.1016/j.fuel.2016.10.055

[16] Laskowski P, Zimakowska-Laskowska M, Matej J, Wiśniowski P. The problem of cold start emissions from vehicles. Combust Engines. 2024; 199(4): 43-51. https://doi.org/10.19206/CE-186471

[17] Li H, Andrews GE, Savvidis D, Daham B, Ropkins K, Bell M, et al. Study of thermal characteristics and emissions during cold start using an on-board measuring method for modern SI car real world urban driving. SAE Int J Engines. 2009; 1(1): 804-19. https://doi.org/10.4271/2008-01-1307

[18] Pielecha J, Magdziak A, Brzezinski L. Nitrogen oxides emission evaluation for Euro 6 category vehicles equipped with combustion engines of different displacement volume. IOP Conf. Ser.: Earth Environ. Sci. 2019; 214: 012010. https://doi.org/10.1088/1755-1315/214/1/012010

[19] Joshi A. Progress and outlook on gasoline vehicle after treatment systems. Johnson Matthey Technol. Rev. 2017; 61: 311-25. https://doi.org/10.1595/205651317X696306

[20] Nandi S, Chaillou C, Dujardin C, Granger P, Laigle E, et al. Evaluating Different Strategies to Minimize cold-start Emissions from Gasoline Engines in steady-state and Transient Regimes. Top Catal. 2022; 66(13-14): 1122-1135. https://doi.org/10.1007/s11244-022-01721-3

[21] Li Y, Liu Z, Li Y, Chen Y, Bai Z, Jing H, Zhang R, Chen J. Influencing Factors and Purification Performance of a Negative Ion Air Purifier for Indoor Ammonia Gas Removal. Buildings. 2025; 15(2): 261. https://doi.org/10.3390/buildings15020261

[22] Kim KH, Szulejko JE, Kumar P, Kwon EE, Adelodun AA, Reddy PAK. Air ionization as a control technology for off-gas emissions of volatile organic compounds. Environmental Pollution. 2017; 225: 729-743. https://doi.org/10.1016/j.envpol.2017.03.026

[23] Islamov RS. An analytical model of the ionic wind in a regular ultracorona. J Phys D: Appl Phys. 2013; 46(37): 375204. https://doi.org/10.1088/0022-3727/46/37/375204

[24] Jang KH, Seo SW, Kim DJ. Electric Field Analysis on the Corona Discharge Phenomenon According to the Variable Air Space between the Ionizer and Ground Current Collector. Appl Syst Innov. 2023; 6(1): 10. https://doi.org/10.3390/asi6010010

[25] Elaissi S, Alsaif NAM, Moneer EM, Gouadria S. Ozone Generation Study for Indoor Air Purification from Volatile Organic Compounds Using a Cold Corona Discharge Plasma Model. Symmetry. 2025; 17(4): 567. https://doi.org/10.3390/sym17040567

[26] Takahashi K, Takaki K, Hiyoshi I, Enomoto Y, Yamaguchi S, Nagata H. Development of a Corona Discharge Ionizer Utilizing High-Voltage AC Power Supply Driven by PWM Inverter for Highly Efficient Electrostatic Elimination. In: Modern Applications of Electrostatics and Dielectrics. London: IntechOpen; 2020. https://doi.org/10.5772/intechopen.88352

[27] Lee D, Heywood J. Effects of Secondary Air Injection During Cold Start of SI Engines. SAE Int J Engines. 2010; 3(2): 182-96. https://doi.org/10.4271/2010-01-2124

[28] Tashtoush BM, Al-Nimr MA, Khasawneh MA. A comprehensive review of ejector design, performance, and applications. Appl Energy. 2019; 240: 138-72. https://doi.org/10.1016/j.apenergy.2019.01.185

[29] Liu F. Review on Ejector Efficiencies in Various Ejector Systems. 15th Int. Refrig. Air Cond. Conf.; 2014; West Lafayette, IN. Paper No.: 1533. p. 1-10.

[30] Lodi F, Zare A, Arora P, Stevanovic S, Jafari M, Ristovski Z, Brown RJ, Bodisco T. Engine Performance and Emissions Analysis in a Cold, Intermediate and Hot Start Diesel Engine. Appl Sci. 2020; 10(11): 3839. https://doi.org/10.3390/app10113839

https://doi.org/10.31875/2409-9848.2025.12.07